



OPEN Phytochemical characterization and bioinformatics guided evaluation of antioxidant and cytotoxic effects of *Psoralea bituminosa*

Nour H. Aboalhaja^{1✉}, Rima Hajjo^{1,2,3}, Fatma Afifi⁵, Heba Syaj¹ & Rana Abu-Dahab⁴

Psoralea bituminosa L. (Fabaceae) is a medicinal plant traditionally used for its antimicrobial, antihyperglycemic, and antioxidant effects. This study investigated its anticancer and antioxidant potential using aqueous and methanol extracts. The methanol extract exhibited higher total phenol (81.57 mg/g) and total flavonoid (39.06 mg/g) contents compared to the aqueous extract. Antioxidant activity, assessed via the DPPH assay, showed moderate potency (IC₅₀: 330.77 µg/mL for aqueous- and 348.27 µg/mL for methanol extracts). Notably, the methanol extract demonstrated significant cytotoxicity against multiple cancer cell lines (IC₅₀: 27.73–53.90 µg/mL) particularly against A549, MDA-MB231, and PC3. Liquid chromatography-mass spectrometry (LC-MS) profiling revealed abundant flavonoids and isoflavones such as daidzein, biochanin A, and 7,3'-dimethoxy-5,6,4'-trihydroxyisoflavone in the methanol extract, correlating with its anticancer effects. In contrast, glycosylated flavonoids in the aqueous extract aligned with antioxidant activity. Cheminformatics clustering supported these findings, identifying distinct structural groups with differing drug-likeness scores. Bioinformatics analysis further identified transcriptomic signatures enriched in oxidative phosphorylation and key cancer-related pathways (e.g., TP53, PI3K, NRF2, and MYC), offering mechanistic insight. This integrative approach combining LC-MS, cheminformatics, and bioinformatics provides a cost-effective framework for decoding phytochemical bioactivity and guiding natural product-based drug discovery.

Keywords *Psoralea bituminosa*, Cytotoxicity, LC-MS, Chemo-profiling, Chem-bioinformatics.

The genus *Psoralea* (family Fabaceae) encompasses over 100 species distributed worldwide¹. *Psoralea bituminosa* L., also known as *Bituminaria bituminosa* (L.) C. H. Stirt. (Fabaceae), is a perennial herbaceous plant, found in South Africa, America, Australia, and in the Mediterranean region. This species is commonly referred to as the Arabian pea, pitch trefoil, or scurf pea². *P. bituminosa* thrives in a variety of soil types, ranging from shallow, stony soils to deep, sandy substrates. It requires full sunlight and well-drained soil, conditions that allow the plant to remain green throughout the summer, making it one of the few species capable of such resilience^{3,4}. The plant's leaves are composed of three unequal leaflets that transition in color from green to grey. Its violet, pea-like flowers bloom between January and June, though the plant can flower year-round in milder climates⁵.

Traditionally, the leaves and legumes of *P. bituminosa* are used as feed for goats and cattle. In herbal medicine, the plant is employed to treat urinary infections, fever, spasms, and epilepsy^{6,7}. In Ayurvedic practices, it serves as an anthelmintic and diuretic⁸. A decoction of the leaves is also applied as a remedy for hair loss¹.

P. bituminosa has attracted considerable pharmacological interest due to its diverse secondary metabolites. Among them are two natural furanocoumarins, psoralen and its angular isomer angelicin, known for their antibacterial and antifungal activity, as well as their applications in the treatment of skin diseases⁹. Other

¹Department of Pharmaceutical Sciences, Faculty of Pharmacy, Al-Zaytoonah University of Jordan, Amman, Jordan. ²Laboratory for Molecular Modeling, Division of Chemical Biology and Medicinal Chemistry, Eshelman School of Pharmacy, The University of North Carolina at Chapel Hill, Chapel Hill, NC, USA. ³Board Member, Jordan CDC, Amman, Jordan. ⁴Department of Pharmaceutics and Pharmaceutical Technology, School of Pharmacy, The University of Jordan, Amman, Jordan. ⁵Department of Pharmaceutical Sciences, School of Pharmacy, The University of Jordan, Amman, Jordan. ✉email: n.aboalhaja@zu.edu.jo

Extract type	Total phenolic content (mg GAE/g)	Total flavonoid content (mg rutin/g)	Antioxidant activity IC ₅₀ (µg/mL)
Aqueous extract	75.16 ± 10.14	10.56 ± 3.19	330.77 ± 10.14
Methanol extract	81.57 ± 2.21	39.06 ± 0.79	348.27 ± 13.21
Ascorbic acid (standard)	–	–	5.51 ± 0.31

Table 1. Total phenol content, total flavonoid content, and antioxidant activity (IC₅₀) of different extracts. Data are expressed as mean ± standard deviation (SD) of triplicate measurements (n = 3).

Cell Line	Aqueous extract	Methanol extract	Doxorubicin
A549	83.47 ± 2.39	13.7 ± 3.97	0.56 ± 0.40
MCF-7	94.81 ± 1.93	27.35 ± 2.94	0.47 ± 0.08
HCT116	95.21 ± 1.31	34.88 ± 2.98	0.74 ± 0.26
DU145	93.87 ± 1.95	37.88 ± 3.14	1.01 ± 0.31
PC3	96.72 ± 2.80	39.15 ± 4.61	0.82 ± 0.01
MDA-MB231	82.32 ± 2.38	41.83 ± 2.58	1.08 ± 0.20
T47D	96.38 ± 2.78	65.04 ± 1.98	0.32 ± 0.01
Fibroblast	> 500	> 500	0.31 ± 0.01

Table 2. Cell viability (%), (mean ± SD) of 100 µg/ml of *P. bituminosa* methanol and aqueous extracts tested on eight types of cell lines (MCF7, MDA-MB231, PC3, DU145, HCT, A549, T47D and fibroblast cells).

notable bioactive compounds include plicatin B, genistein, daidzin, 8-prenyldaidzein, iso-orientin, apigenin, phenolic acids, lignans and saponins⁷. These constituents contribute to the plant’s potential for pharmaceutical development.

The present study aimed to investigate phytochemically the aqueous and methanol extracts of *P. bituminosa*, which grows wild in Jordan, and to evaluate their antiproliferative activity against a panel of cancer cell lines. Additionally, bioinformatics tools were applied to analyze the gene expression profiles of the cancer cell lines and to uncover the associated signaling pathways involved in their response. By assessing the chemical composition, antioxidant activity, and cytotoxic effects of the aqueous and methanol extracts, this study will provide insights into the bioactive properties of the plant’s phytochemicals and their potential as therapeutic agents for cancer treatment.

Results

Total phenol, total flavonoid content and antioxidant activity

The total phenol content (TPC), total flavonoid content (TFC), and antioxidant activity of the aqueous and methanol extracts of *P. bituminosa* are presented in Table 1. Antioxidant activity was evaluated using the DPPH assay, and the IC₅₀ values indicate the extract concentration required to scavenge 50% of the DPPH radicals.

Earlier Ayoubi et al., (2018) reported higher TPC and TFC values for the methanol extract of *P. bituminosa*, collected in Israel¹⁰. These discrepancies may be explained by the differences in biogeography, seasonal variation, and experimental protocols, all of which influence the phytochemical composition of plant extracts^{11,12}.

Antiproliferative evaluation

The antiproliferative effects of the aqueous and methanol extracts were evaluated against eight cancer cell lines: A549, MCF7, HCT116, DU145, PC3, MDA-MB231, T47D, and one fibroblast cell line (Table 2; Fig. 1). At a screening concentration of 100 µg/mL, the methanol extract demonstrated notable cytotoxicity, particularly against A549 (13.7 ± 3.97%), MCF7 (27.35 ± 2.94%), and MDA-MB231 (41.83 ± 2.58%) cell lines. In contrast, the aqueous extract exhibited minimal cytotoxic effects, with cell viability remaining relatively high in A549 (83.47 ± 2.39%) and MCF7 (94.81 ± 1.93%) cell lines.

Cell viability assay results (Table 2) revealed that the methanol extract of *P. bituminosa* induced significantly greater cytotoxicity across all tested cancer cell lines compared to the aqueous extract, indicating a stronger antiproliferative effect of the methanol fraction.

Based on the cytotoxic effect observed with the methanol extract, IC₅₀ values were determined only for this extract, which exhibited varying potency across the all-tested cancer cell lines tested (Fig. 2). The IC₅₀ values ranged from 27.73 µg/mL for A549 cells to over 150 µg/mL for T47D cells, indicating differential cellular sensitivity. These variations may reflect differences in cancer cell type, passage number, and intrinsic resistance mechanisms. A549 cells were the most sensitive to the methanol extract, while T47D cells exhibited the highest resistance.

Liquid chromatography-mass spectrometry (LC-MS) analysis

The LC-MS analysis of the aqueous and methanol extracts revealed a diverse array of bioactive compounds potentially responsible for the observed biological activities (Table 3).

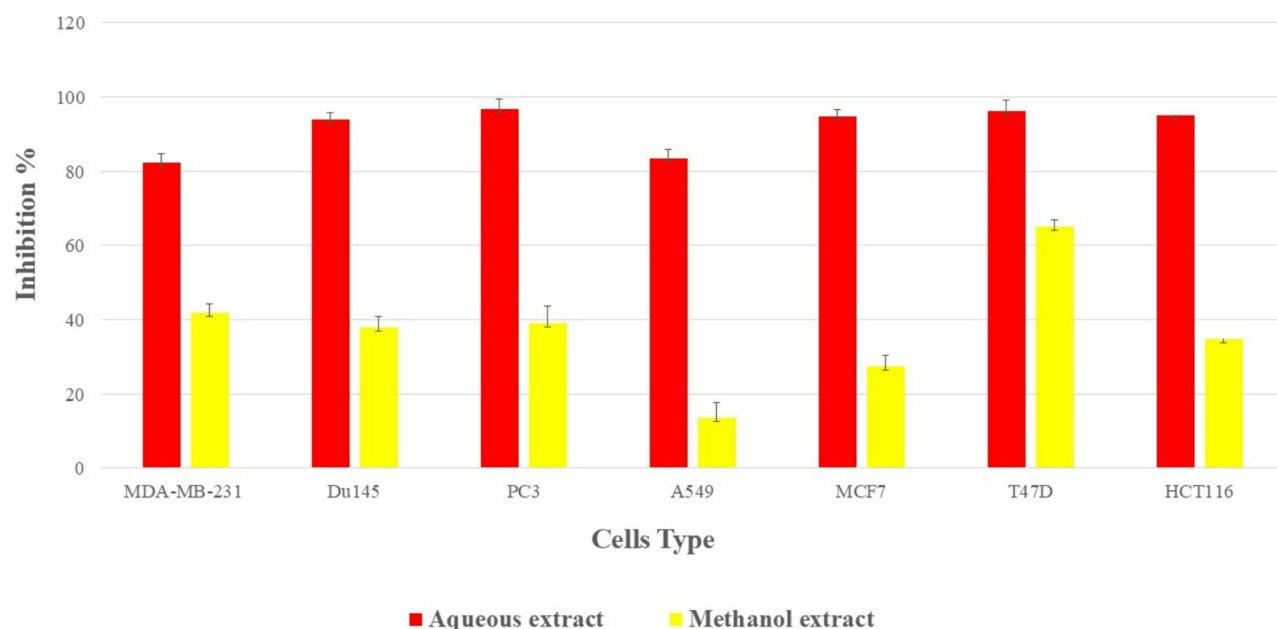


Fig. 1. Cell viability (%) of 100 µg/ml of *P. bituminosa* methanol and aqueous extracts on MCF7, MDA-MB231, PC3, DU145, HCT, A549, T47D and Fibroblast cells.

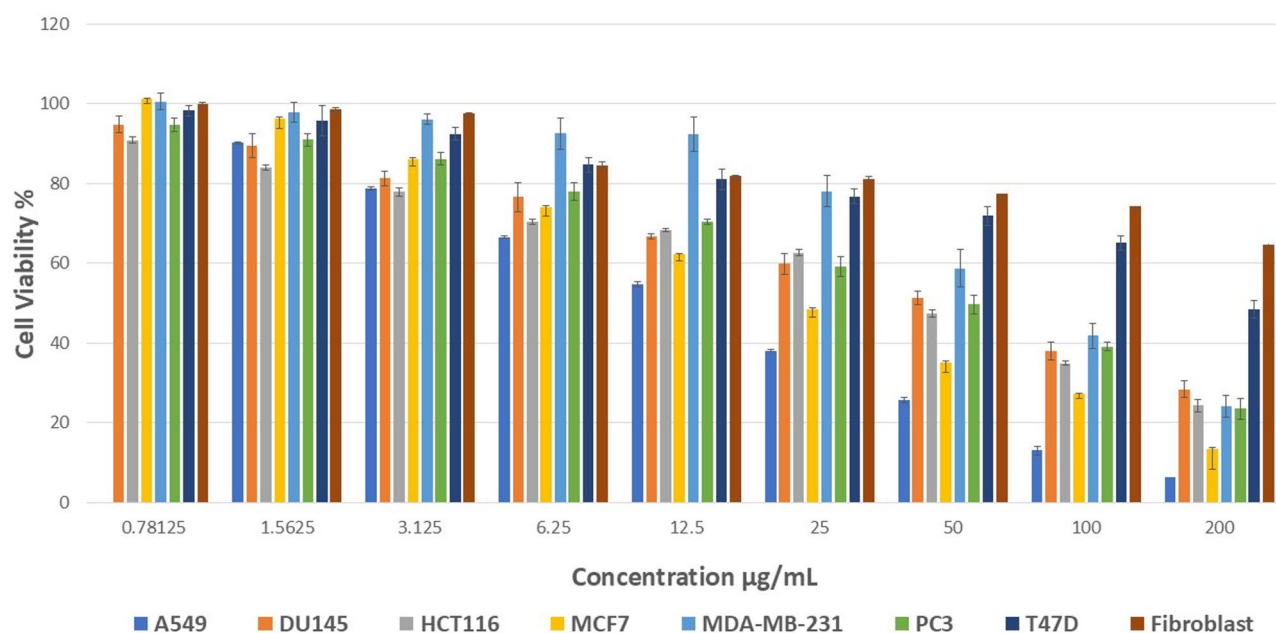


Fig. 2. Antiproliferative effect of *P. bituminosa* methanol extracts on MCF7, MDA-MB231, PC3, DU145, HCT116, A549, T47D and Fibroblast. Mean \pm SD, $n = 3$.

The LC-MS analysis of both aqueous and methanol extracts revealed a diverse profile of bioactive phytochemicals, including phenolic acids, flavonoids, coumarins, and isoflavones, which may underlie the extracts' anticancer activity. The aqueous extract was particularly rich in flavonoid glycosides, with high levels of iso-orientin (26.89%), vitexin (25.62%), and saponarin (8.51%), as well as notable amounts of caffeic acid (13.36%) and the hydroxycoumarin aesculetin (5.71%). In contrast, the methanol extract exhibited elevated concentrations of isoflavones, including daidzein (20.15%), biochanin A (19.28%), and 7,3'-dimethoxy-5,6,4'-trihydroxyisoflavone (13.70%), in addition to benzoic acid (9.98%) and catechol (10.46%).

No.	RT [min]	Name	Molecular formula	M.Wt	Ion type	Aqueous extract		Methanolic extract		Ref. no.
						AUC	% within identified	AUC	% within identified	
1	1.83	Succinic acid	C ₄ H ₆ O ₄	118.09	[M+H] ⁺	2436	1.30	–	–	13,14
2	3.09	4-Hydroxybenzoic acid	C ₇ H ₆ O ₃	138.12	[M+H] ⁺	2576	1.37	180	0.05	13,14
3	3.16	Pivalic Acid	C ₅ H ₁₀ O ₂	102.13	[M+H] ⁺	4954	2.64	–	–	15
4	3.29	2,5-Dihydroxybenzoic acid	C ₇ H ₆ O ₄	154.12	[M+H] ⁺	1574	0.84	–	–	14
5	3.39	Adenosine	C ₁₀ H ₁₃ N ₅ O ₄	267.24	[M+H] ⁺	5816	3.10	–	–	16
6	3.83	<i>p</i> -Coumaric acid	C ₉ H ₈ O ₃	164.16	[M+H] ⁺	9210	4.91	–	–	13,14,17
7	4.12	Vanillic acid	C ₈ H ₈ O ₄	168.15	[M+H] ⁺	–	–	4784	1.41	14
8	4.17	Caffeic Acid	C ₉ H ₈ O ₄	180.16	[M+H] ⁺	25,050	13.36	–	–	14,18
9	4.19	Vanillin	C ₈ H ₈ O ₃	152.15	[M+H] ⁺	932	0.50	–	–	19
10	4.19	Aesculetin	C ₉ H ₆ O ₄	178.14	[M+H] ⁺	10,698	5.71	4402	1.29	14
11	4.37	Iso-orientin	o	448.37	[M+H] ⁺	50,400	26.89	3786	1.11	13
12	4.43	Benzoic acid	C ₇ H ₆ O ₂	122.12	[M+H] ⁺	–	–	33,962	9.98	14
13	4.58	Saponarin	C ₂₇ H ₃₀ O ₁₅	610.51	[M+H] ⁺	15,948	8.51	–	–	20
14	4.62	Vitexin	C ₂₁ H ₂₀ O ₁₀	432.37	[M+H] ⁺	48,234	25.62	2522	0.74	13
15	4.63	Scopoletin	C ₁₀ H ₈ O ₄	192.17	[M+H] ⁺	212	0.11	984	0.29	16
16	4.83	Salicylic acid	C ₇ H ₆ O ₃	138.12	[M+H] ⁺	–	–	5662	1.66	14
17	5.14	Apigenin	C ₁₅ H ₁₀ O ₅	270.24	[M+H] ⁺	–	–	1720	0.51	16
18	5.23	Ferulic acid	C ₁₀ H ₁₀ O ₄	194.18	[M+H] ⁺	4434	2.37	20,104	5.91	17
19	5.68	7,3'-Dimethoxy-5,6,4'-trihydroxyisoflavone	C ₁₇ H ₁₄ O ₇	330.29	[M+H] ⁺	–	–	46,614	13.70	21
20	5.71	3,5-Dimethoxy-4-hydroxyacetophenone	C ₁₀ H ₁₂ O ₄	196.20	[M+H] ⁺	–	–	1630	0.48	22
21	5.75	Daidzein	C ₁₅ H ₁₀ O ₄	254.24	[M+H] ⁺	–	–	68,552	20.15	21
22	5.84	Biochanin A	C ₁₆ H ₁₂ O ₅	284.26	[M+H] ⁺	5170	2.76	65,596	19.28	23
23	6.21	3,6,2',4'-Tetrahydroxyflavone	C ₁₅ H ₁₀ O ₆	286.24	[M+H] ⁺	–	–	2670	0.78	17
24	6.92	3',4',7-Trihydroxyisoflavone	C ₁₅ H ₁₀ O ₅	270.24	[M+H] ⁺	–	–	6878	2.02	21
25	7.02	Hispidulin	C ₁₆ H ₁₂ O ₆	300.26	[M+H] ⁺	–	–	4164	1.22	17
26	7.65	Kumatakenin	C ₁₇ H ₁₄ O ₆	314.29	[M+H] ⁺	–	–	24,012	7.06	14
27	8.94	Glycitein	C ₁₆ H ₁₂ O ₅	284.26	[M+H] ⁺	–	–	3652	1.07	14
28	10.53	Catechol	C ₆ H ₆ O ₂	110.11	[M+H] ⁺	–	–	35,576	10.46	24
29	10.87	5,3',4'-Trihydroxyflavone	C ₁₅ H ₁₀ O ₅	270.24	[M+H] ⁺	–	–	2816	0.83	25

Table 3. Identified phytochemicals in the aqueous and methanol extracts of *P. bituminosa* by LC-MS. AUC: area under the curve.

Computational chemical biology studies

Cheminformatics analysis of *P. bituminosa* phytochemicals

The cheminformatics analysis conducted on 47 molecular structures corresponding to the phytochemicals identified in the aqueous and methanol extracts of *P. bituminosa* by LC-MS (Table 3). First, the structural information of all compounds in SMILES format was retrieved from PubChem. The structures were standardized using RDKit²⁶ by applying the following procedures: aromatization, adding explicit hydrogens, generating 2D coordinates, cleaning the molecule for correct stereochemistry, and removing stereochemistry information. 3,885 2D molecular descriptors were generated using alvaDesc²⁷, out of 5,305 available descriptors. Finally, Principal Component Analysis (PCA) was performed using 1,873 molecular descriptors, -after filtering out constant, near-constant, or missing-value descriptors, - to visualize the clustering and distribution of phytochemicals identified in *P. bituminosa* (Fig. 3). This figure presents four PCA-derived clusters based on the molecular descriptors of *P. bituminosa* phytochemicals, highlighting their distribution and potential bioactivity. The bottom-left (negative PC1, PC2) includes flavonoid-rich compounds from the methanol extract such as daidzein (20.15%), biochanin A (19.28%), and 7,3'-dimethoxy-5,6,4'-trihydroxyisoflavone (13.70%). This cluster likely drives the observed methanolic extract's strong anticancer activity. The top left cluster (negative PC1 and positive PC2) consists of glycosylated flavonoids and polyphenols including iso-orientin, vitexin, and saponarin. These are more abundant in the aqueous extract and are associated with antioxidant activity but lower cytotoxicity, possibly due to reduced lipid permeability (as has been reported for glycosides extracted from other plants²⁸). The bottom right cluster (positive PC1 and negative PC2) is enriched with phenolic acids, caffeic acid and aesculetin, along with minor constituents like caffeine, scopoletin, and resveratrol, which have known antioxidant, anti-inflammatory and anticancer properties. The top right cluster (positive PC1 and PC2) contains organic acids, where aromatic acids such as gallic acid and 2,5-dihydroxybenzoic acid have moderate PC2 values, and aliphatic acids such as succinic-, pivalic-, and ascorbic acids with higher PC2 values. Benzoic acid (9.98%), which is abundant in the methanol extract, lies at the boundary between the last two clusters.

In the PCA plot, coordinates representing phytochemicals were color-coded based on their consensus drug-likeness scores (DLS_cons), which reflect the average of seven drug-likeness scoring functions included in the

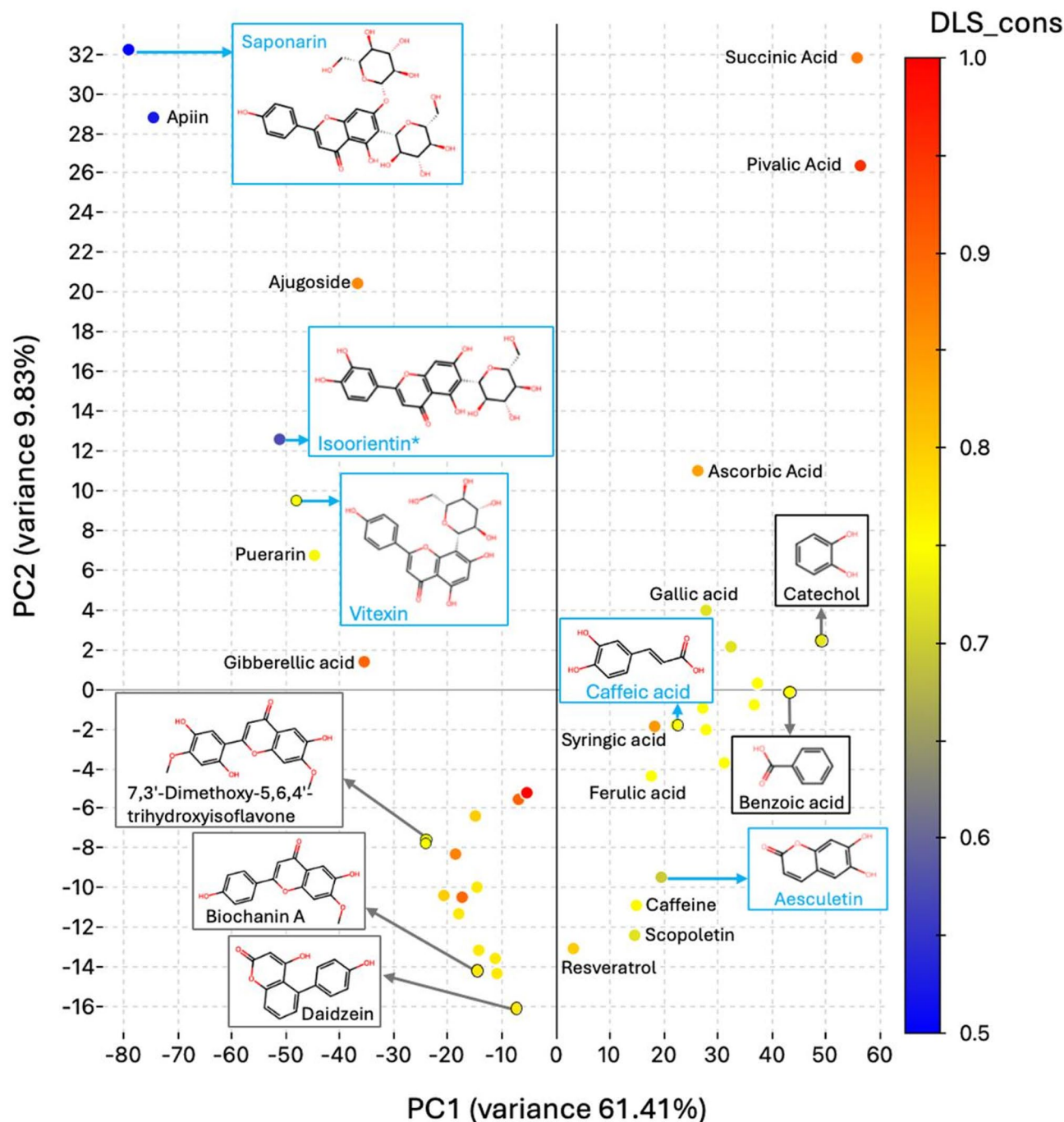


Fig. 3. PCA analysis of phytochemicals identified in *P. bituminosa* extracts. Circles indicating phytochemicals (colored based on their consensus drug-like scores (DLS_cons)). The structures of the major phytochemicals in the methanol extract outlined in black, and structures of the major phytochemicals in the aqueous extract outlined in cyan.

alvaDesc descriptor software. The color gradient ranges from blue (lower DLS) to red (higher DLS), visually indicating the relative drug-likeness of each compound. The DLS_cons values span from 0.0 to 1.0, and all phytochemicals analyzed in this study exhibited scores of 0.50 or higher, suggesting moderate to high drug-like potential.

Bioinformatics analysis of tested cancer cell lines

A bioinformatics analysis of seven cancer cell lines (A549, MCF7, HCT116, DU145, PC3, MDA-MB231, and T47D) was conducted using transcriptomic data from CCLE²⁹ and pathway enrichment data from cBioPortal³⁰. PCA of RNA-seq data revealed that A549 had a distinct gene expression profile, clustering more closely with DU145, HCT116, MCF7, and MDA-MB231, and was most dissimilar to PC3 and T47D (Fig. 4A). This aligned

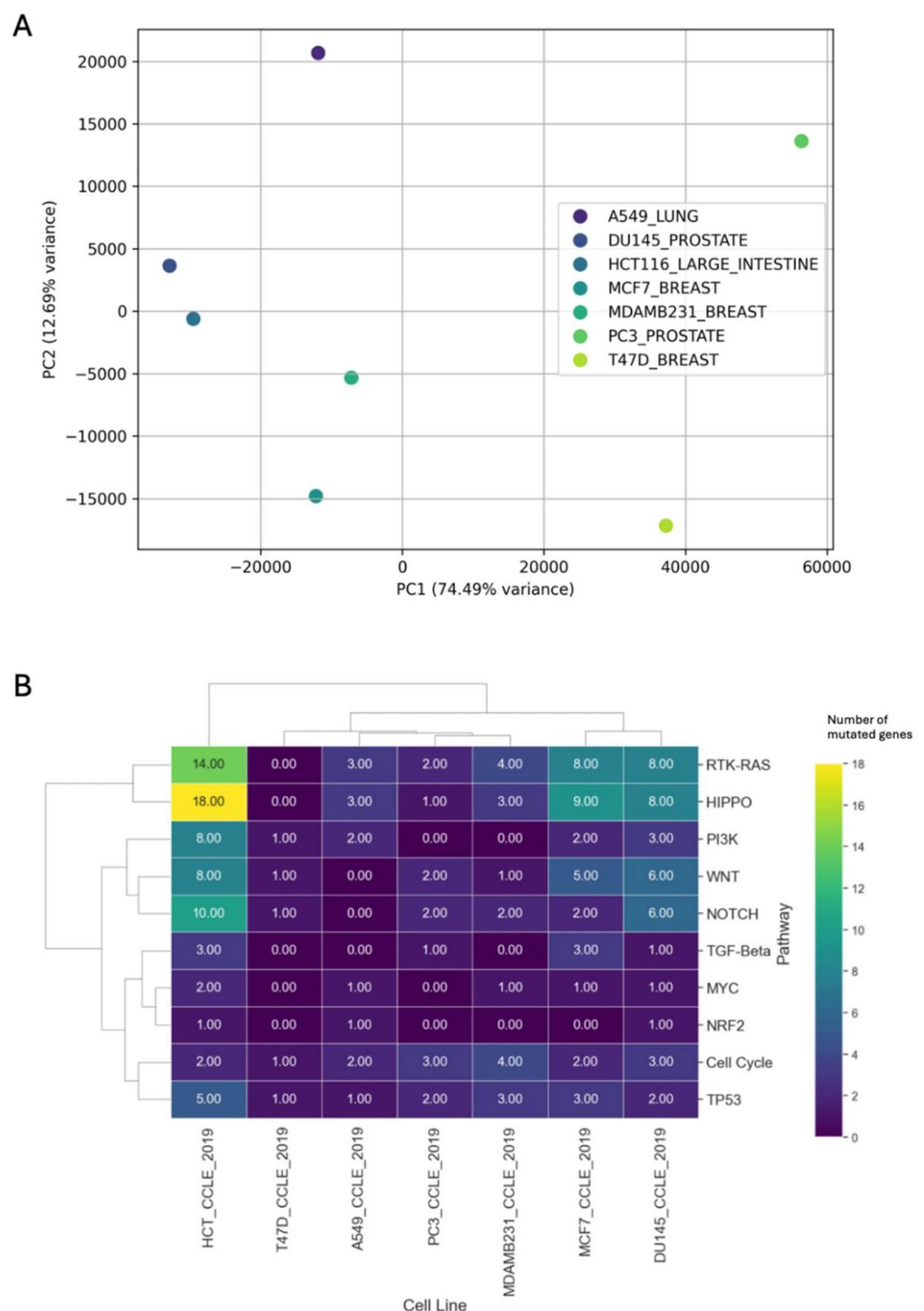


Fig. 4. Visualization of cell line similarity/dissimilarity based on transcriptomics and pathway enrichment data. (A) PCA Analysis of Cancer Cell Lines from CCLE Database. (B) Clustered heatmap based on the number of mutated genes between seven cancer cell lines.

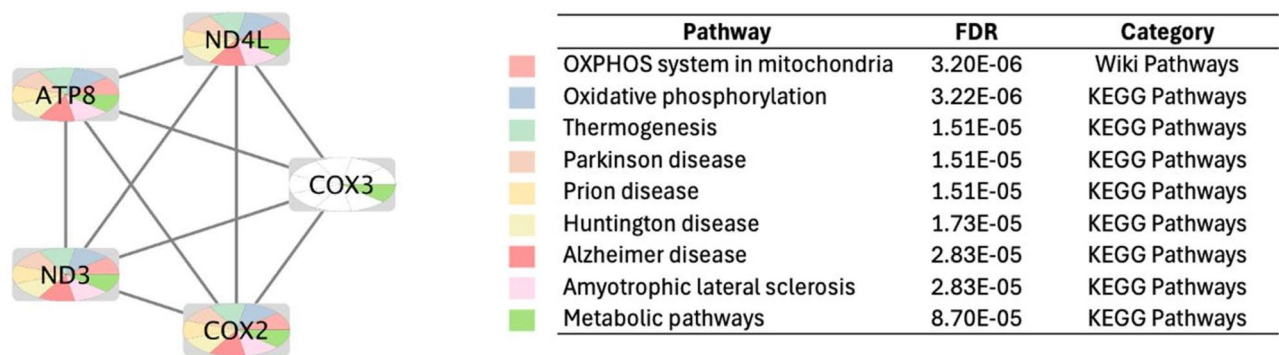


Fig. 5. Protein-protein interactions network for ATP8, ND3, ND4L, COX2 and COX3.

with cytotoxicity results, where A549 was the most sensitive and T47D the most resistant to *P. bituminosa* methanol extract, prompting further exploration of cancer pathway involvement.

Pathway analysis of tested cancer cell lines

Pathway perturbation data for the cancer cell lines were mined from cBioPortal³⁰ using CCLE_2019 dataset of the Cancer Cell Line Encyclopedia (CCLE). A similarity matrix based on the number of mutated cancer genes in 10 key cancer pathways was generated and plotted as a heatmap shown in Fig. 4B. The analyzed 10 cancer pathways included: RTK-RAS, HIPPO, PI3K, WNT, NOTCH, TGF-Beta, MYC, NRF2, cell cycle, and TP53. According to the number of mutated genes in these 10 cancer pathways, DU145 and MCF7 shared highest similarity, and these two cell lines were more similar to HCT than the rest of cell lines consisting of T47D, A549, PC3 and MDA-MB231.

Mechanistic insights

The top genes exhibiting the most significant differential expression between T47D and other cell lines, particularly A549, included ATP8, ND3, ND4L, COX2, and COX3. To explore the functional implications of these genes, their protein-protein interaction (PPI) networks were constructed, incorporating both the genes themselves and their nearest neighbor proteins/genes. Subsequently, biological pathway enrichment analysis was performed to identify key pathways associated with these network genes, as illustrated in Fig. 5.

The pathway enrichment analysis revealed an association with oxidative phosphorylation (OXPHOS), a critical process that couples the electron transport chain (ETC) to ATP generation. OXPHOS plays a pivotal role in cancer biology, as cancer cells exploit ETC and OXPHOS to meet their heightened energy demands, resist oxidative stress, and support proliferation, metastasis, and apoptosis resistance. Beyond cancer, OXPHOS has been also linked to neurodegenerative diseases (e.g., Parkinson's, Huntington's, Alzheimer's, and ALS), thermogenesis, and prion diseases. Notably, OXPHOS intersects with several other critical pathways such as MYC, NRF2, TP53, PI3K, and the cell cycle, which may collectively contribute to the anticancer activity of the methanol extract of *P. bituminosa*.

Mining the biomedical literature for supportive evidence

These findings were in line with previous studies on *Psoralea* species, highlighting their cytotoxic potential. For example, a study in Korea revealed that ripe fruits of *P. corylifolia* inhibited several colorectal cancer cell lines including SW480 (IC₅₀: 37.9 µg/mL), HT-29 (IC₅₀: 40.7 µg/mL), and HCT116 (IC₅₀: 45.3 µg/mL), by downregulating cyclin D1 and CDK4 expression³¹. Another study from Ireland demonstrated antiproliferative activity of *P. corylifolia* ethanol extract against HEp-2 cells (IC₅₀: 22 µg/mL), A549 cells (IC₅₀: 68 µg/mL)³². Similarly, a study in China revealed that *P. corylifolia* methanol extract exhibited potent growth inhibition in KB, KBv200, K562, and K562/ADM cells, with IC₅₀ values ranging from 10.0 to 26.9 µg/mL. In India, *P. corylifolia* seed extract was found to induce apoptosis in human breast cancer MCF-7 cells³³. In Italy, a chloroform extract of *P. bituminosa* leaves, shoots, and roots demonstrated cytotoxic activity against HeLa cells, with the highest cytotoxicity observed in the shoots³⁴.

Daidzein and biochanin A, the two most abundant phytochemicals in the methanol extract, are known for their cytotoxic effects against hormone-dependent cancers, which align with the observed potent activity against breast and prostate cancer cell lines. Biochanin A has demonstrated cytotoxicity against A549 lung cancer cells^{35–38}. Additionally, ferulic acid and benzoic acid, both present in significant concentrations, may contribute to the extract's pro-apoptotic and antioxidant properties^{39,40}. On the other hand, the aqueous extract exhibited weaker cytotoxicity, as evidenced by its higher IC₅₀ values, likely due to the prevalence of flavonoid glycosides, which may have reduced cellular uptake and bioavailability compared to their aglycone counterparts. The limited anticancer effects of the aqueous extract suggest that glycosylation plays a role in modulating the bioactivity of these compounds.

One study provided indirectly supported the mechanistic insights identified in this study linking OXPHOS to the cytotoxic effects of *P. bituminosa*. It revealed that 7,3,4'-trihydroxyisoflavone (THIF), a metabolite of daidzein (the major phytochemical in the methanol extract of *P. bituminosa*), inhibits UVB-induced cyclooxygenase-2

(COX-2) expression by suppressing NF- κ B transcriptional activity⁴¹. THIF directly inhibits Cot and MKK4 kinase activities, reducing the phosphorylation of mitogen-activated protein kinases (MAPKs). This result aligns well with the finding that COX2 was among the top differentially expressed genes in cancer cell lines most responsive to the methanolic extract, further supporting its association with OXPHOS pathways.

Discussion

P. bituminosa, a medicinal plant traditionally used for various ailments, has recently gained considerable attention due to its broad pharmacological potential. In this study, we comprehensively evaluated the antioxidant and anticancer activities of both methanolic and aqueous extracts of *P. bituminosa*, using an integrated experimental and computational approach.

The antioxidant assays revealed that both extracts exhibit moderate to strong activity, in line with their high total phenolic and flavonoid content, as quantified by Folin-Ciocalteu and aluminum chloride assays. These findings are corroborated by LC-MS analysis, which confirmed the presence of potent antioxidant constituents, including flavonoids, phenolic acids, and coumarins. Evidence from biomedical literature reaffirmed the putative antioxidant potential of the aqueous extract of *P. bituminosa*^{42,43}.

The methanolic extract, however, demonstrated superior cytotoxicity, with the most potent effects observed against the A549 lung cancer cell line, followed by MDA-MB231 (breast) and PC3 (prostate). The enhanced activity is likely due to the presence of lipophilic isoflavones (daidzein, biochanin A) and phenolic acids, which can cross cellular membranes more efficiently and exert intracellular effects. These compounds are known to modulate multiple cancer-related pathways, including estrogen receptor signaling, apoptosis induction, and cell cycle arrest, possibly through ROS generation and mitochondrial depolarization⁴⁵.

The redox properties of phenolics and flavonoids not only confer antioxidant protection but also play a dual role in cancer, where at higher concentrations they may induce oxidative stress selectively in tumor cells. This pro-oxidant mechanism is particularly relevant in flavonoid-rich methanolic extracts, supporting their selective cytotoxicity. Such biphasic behavior underscores the therapeutic promise of flavonoids as redox modulators in cancer.

The computational chemical biology studies unveiled the structural diversity and physicochemical properties of *P. bituminosa* phytochemicals. Using cheminformatics tools, a total of 47 phytochemicals with drug-like properties were analyzed. The drug-likeness of these compounds was quantified using consensus DLSs generated by alvaDesc. Notably, most of the analyzed phytochemicals exhibited high DLSs, suggesting favorable absorption, distribution, metabolism, and excretion profiles. In contrast, flavonoid glycosides, which contain sugar moieties, scored lower, likely due to their increased polarity, higher molecular weight, and reduced membrane permeability. This highlights how structural differences, such as the presence of glycosidic groups/sugar molecules, can influence drug-like behavior and potentially modulate biological activity—a finding consistent with the reduced cytotoxicity often observed for highly glycosylated flavonoids. Principal Component Analysis (PCA) further underscored the physicochemical diversity of these compounds, emphasizing their potential bioactivity and aligning with their putative therapeutic applications.

The cheminformatics characterization of *P. bituminosa* phytochemicals using 2D alvaDesc molecular descriptors and PCA-based clustering identified four unique clusters and results were well-aligned with the experimental findings. The anticancer properties of the methanolic extract are likely driven by flavonoids as evidenced by the clustering of the three major phytochemicals—daidzein, biochanin A, and 7,3'-Dimethoxy-5,6,4'-trihydroxyisoflavone—within a distinct group. These features are commonly associated with enhanced cellular uptake and interaction with intracellular targets such as estrogen receptors and apoptotic regulators. Meanwhile, the antioxidant effects of the aqueous extract primarily arise from glycosylated flavonoids and polyphenolic compounds (e.g., hydroxylated coumarins and phenolic acids) which are generally more hydrophilic and exert their effects through extracellular radical scavenging and modulation of redox-sensitive pathways. Interestingly, the majority of phytochemical constituents of *P. bituminosa* exhibit acceptable drug-like properties, as indicated by DLS above 0.7. However, the lowest scores were observed for flavonoid glycosides, including apiin, isoorientin, and saponarin, which had scores closer to 0.5—the midpoint of the 0.0 to 1.0 DLS_{cons} range. This reduction in drug-likeness is likely due to their increased hydrophilicity, decreased membrane permeability, and reduced interaction with lipophilic binding pockets in protein targets. These findings provide a structural/molecular basis for further research and the therapeutic exploration of bioactive phytochemicals.

Bioinformatics analyses of seven cancer cell lines (A549, MCF7, HCT116, DU145, PC3, MDA-MB231, and T47D) indicated distinct transcriptomic profiles that correlated with differential sensitivity to *P. bituminosa* extracts. Lung cancer cell line A549 exhibited strong sensitivity to the methanolic extract, while breast cancer cell line T47D (breast cancer) demonstrated resistance. Enrichment analysis of key genes identified from the bioinformatics analysis of cancer cell lines revealed pathways centered on oxidative phosphorylation (OXPHOS), a key metabolic process that supports cancer proliferation and survival. The findings underscore how *P. bituminosa*'s phytochemicals may target cancer pathways associated with NRF2, TP53, and PI3K, with potential effects on MYC, suggesting their promise for therapeutic development. Evidence from the biomedical literature indicates that phytochemicals, generally, have been shown to influence cancer pathways associated with genes such as NRF2, TP53, and PI3K. However, while MYC is a well-known modulator of cell proliferation and metabolism in cancer, there is limited direct evidence demonstrating that phytochemicals specifically target MYC-driven pathways. Thus, this gap presents an opportunity for experimental investigation by interested researchers including pharmacologists, cancer biologists, molecular biologists, biochemists, and other researchers exploring the therapeutic potential of phytochemicals in MYC-driven cancer pathways.

These findings align with previous studies on *Psoralea* species, demonstrating cytotoxic effects against various cancer cell lines, including colorectal (IC₅₀: 37.9–45.3 μ g/mL)³¹, HEP-2 (IC₅₀: 22 μ g/mL), and A549 (IC₅₀: 68 μ g/mL)³², as well as MCF-7 and HeLa cells^{33,34}. Key compounds like daidzein, biochanin A, ferulic acid,

and benzoic acid contribute to pro-apoptotic and antioxidant activities^{35–40}. These results further highlight the role of glycosylation in modulating bioactivity and the therapeutic potential of *Psoralea* species.

In conclusion the integrative approach combining computational chemical biology and experimental pharmacological studies characterized the anticancer and antioxidant properties of *P. bituminosa* and identified this medicinal plant as a promising source of anticancer compounds, particularly against lung cancer. The presence of bioactive flavonoids such as daidzein, Biochanin A, and 7,3'-Dimethoxy-5,6,4'-trihydroxyisoflavone is likely responsible for these effects. In contrast, the aqueous extract, which is rich in glycosylated flavonoids and polyphenolics, showed strong antioxidant activity but lower cytotoxicity, suggesting a protective role rather than a therapeutic one in cancer. Cheminformatics and bioinformatics analyses further linked the anticancer effects to key metabolic and signaling pathways, including oxidative phosphorylation (OXPHOS), NRF2, TP53, PI3K, and MYC. These findings emphasize the importance of solvent selection in maximizing the extraction of bioactive compounds and highlight *P. bituminosa* as a promising source of therapeutic agents for cancer and potentially other diseases related to oxidative stress and metabolism. Future research should prioritize isolating active compounds, elucidating their mechanisms of action, and optimizing bioavailability for clinical applications, particularly in cancer therapy.

Materials and methods

Preparation of plant extracts

The aerial parts of *P. bituminosa* were collected from surroundings of Amman, the capital of Jordan (31°N, 35°E), located in the Mediterranean biogeographic zone of Jordan⁴⁴. The plant was identified by Prof. Fatma Afifi using descriptive references and by comparison with the herbarium species from the School of Science, The University of Jordan^{5,45}. A voucher specimen of *P. bituminosa* has been deposited in the Department of Pharmaceutical Sciences, School of Pharmacy, The University of Jordan, under the deposition number FMJ-PB-02. The fresh plant material was finely chopped and divided into two portions, then subjected to maceration using water and methanol, respectively, at room temperature in the dark for one week. Following solvent evaporation using a rotary evaporator, the resulting crude extracts were stored in refrigerator until further analysis.

Determination of total phenol

A one mL aliquot of each extract (1 mg/mL) was diluted with 10 mL of distilled water. After five minutes, 200 µL of Folin-Ciocalteu reagent was added, followed by 800 µL of 20% sodium carbonate. The volume was adjusted to 5 mL with distilled water, and the mixture was incubated in the dark at room temperature for one hour. Absorbance was then measured at 765 nm. Gallic acid was used as the standard at concentrations of 100, 50, 25, 12.5, and 6.125 µg/mL. All measurements were performed in triplicate⁴⁶.

Determination of flavonoids content

Two milliliters of the extract (1 mg/mL) were mixed with 0.1 mL of 10% aluminum chloride (AlCl₃), 100 µL of 1 M sodium acetate, and 2.8 mL of distilled water. The mixture was incubated at room temperature for 30 min, and the absorbance was measured at 415 nm. Rutin was used as the standard, and methanol served as the blank⁴⁷.

Antioxidant activity determination

The antioxidant activity of the extracts was assessed using the DPPH (2,2-diphenyl-1-picrylhydrazyl) free radical scavenging assay. A 0.1 mM DPPH solution in methanol (40 µL) was added to 250 µL of plant extract at serial concentrations (1–500 µg/mL) in a 96-well plate. The control consisted of methanol. After 30 min of incubation at room temperature, absorbance was measured at 517 nm. Trolox was used as the standard, and DPPH inhibition was calculated using the following formula:

$$I\% = (\text{OD}_{\text{control}} - \text{OD}_{\text{sample}}) / \text{OD}_{\text{control}} \times 100\%$$

where OD_{control} and OD_{sample} are the optical densities of the control and the sample, respectively.

Antiproliferative assay

The antiproliferative activity of the *P. bituminosa* extracts was evaluated using the MTT assay, following the previously described method⁴⁴. Briefly, cells were seeded in 96-well plates. Treated with varying concentrations (3.9–500 µg/mL) of the extract for 72 h. Cell viability was calculated using the following formula:

$$\text{Cell viability (\%)} = (\text{OD}_{\text{treated cells}} / \text{OD}_{\text{control cells}}) \times 100\%$$

The IC₅₀ values were calculated by plotting cell viability against extract concentration. Doxorubicin (50 mg/25 mL) was used as a positive control.

LC-MS analysis

The chemical composition of the methanolic extract was analyzed using a Bruker Daltonik Impact II ESI-Q-TOF mass spectrometer (Bremen, Germany) coupled with a Bruker Daltonik Elute UPLC system. Chromatographic separation was achieved using a Bruker Solo 2.0_C18 UHPLC column (100 mm × 2.1 mm, 2.0 µm particle size) maintained at 40 °C. The flow rate was set to 0.51 mL/min with a total run time of 30 min. The injection volume was 3 µL.

The mobile phases consisted of solvent A (water containing 0.1% formic acid) and solvent B (methanol). Gradient elution was used for optimal separation. The ionization was performed using an Apollo II ion funnel electrospray (ESI) source operated in positive mode. The MS parameters were as follows: capillary voltage,

2500 V; nebulizer gas pressure, 2.0 bar; dry gas (nitrogen) flow, 8 L/min; dry temperature, 200 °C; mass resolution, 50,000 FSR; mass accuracy, <1 ppm; and TOF repetition rate, up to 20 kHz. For identification, standard compounds were used to determine both the exact *m/z* values and retention times⁴⁸. All solvents used (acetonitrile, methanol, water, and formic acid) were LC/MS grade.

Sample preparation

Stock solutions of reference compounds were prepared by dissolving appropriate amounts in DMSO (analytical grade) and diluting with acetonitrile. For analysis, unknown samples were dissolved in 2.0 mL of methanol and centrifuged at 4000 rpm for 2.0 min. A 1.0 mL aliquot of the supernatant was transferred to the autosampler vial, and 3.0 µL was injected for LC-MS analysis.

Computational methods

Integrative chemical biology informatics approach

An integrative informatics workflow adapted from Hajjo et al.^{49–52}, was applied to investigate the network pharmacology and anticancer mechanisms of *P. bituminosa*. This workflow includes: (1) a cheminformatics module to assess the chemical diversity and predicted activities of its phytochemicals; (2) a network-mining module to identify genetic perturbations in relevant cancer cell lines; and (3) a pathway enrichment module to elucidate biological processes underlying its anticancer effects.

Molecular descriptors

Molecular descriptors quantify the physicochemical properties of molecules. In this study, 2D alvaDesc²⁷ molecular descriptors were generated for 47 *P. bituminosa* phytochemicals, whose structures were retrieved from PubChem in SMILES format and standardized following Hajjo et al.^{49–52}. Out of 5305 descriptors, 3885 2D descriptors were calculated, and 1873 were retained for PCA after removing invariant, incomplete, or low-variance descriptors^{49–52}.

Protein-protein interactions

Functional protein-protein interaction networks for key genes identified from studying the genetic perturbations in cancer lines were generated in Cytoscape version 3.10.1 using the StringApp⁵³.

Enrichment analysis

Pathway enrichment analysis was conducted using Cytoscape StringApp⁵³. The genes/proteins of the generated functional protein-protein interaction network were used as query seeds for the enrichment analysis. The significance of the enrichment results was assessed by calculating the false discovery rates (FDRs) of the hypergeometric *p*-values. Pathways with FDR values below the threshold of 0.05 were classified as statistically significant and relevant to the gene list under investigation.

Cancer cell line encyclopedia (CCLE) database

The CCLE, a joint effort between the Broad Institute and the Novartis Institutes for Biomedical Research, provides comprehensive molecular profiles for 1,072 cell lines derived from diverse lineages and ethnic backgrounds. It serves as a robust resource for studying genetic alterations, identifying drug targets, and exploring small-molecule and biologic therapies. Herein, gene-level RNA-seq data in TPM (Transcripts Per Million) format were retrieved for A549, MCF7, HCT116, DU145, PC3, MDA-MB231, and T47D cell lines. The TPM normalization accounts for both gene length and sequencing depth, similarly to RPKM, to ensure that the total expression levels across samples are comparable. These data were used for the PCA analysis of cancer cells lines, as well as pathway enrichments mined from cBioPortal³⁰.

Statistical analysis

Data were expressed as mean ± standard deviation (SD) of three independent experiments. Statistical analyses were performed using SPSS (version 22). One sample t-tests, one-way analysis of variance (ANOVA), and Tukey's test were used to assess the statistical significance between the groups. A *p*-value ≤ 0.05 was considered statistically significant.

Data availability

All data generated or analysed during this study are included in this published article.

Received: 17 February 2025; Accepted: 26 May 2025

Published online: 30 May 2025

References

- Bertoli, A., Menichini, F., Noccioli, C., Morelli, I. & Pistelli, L. Volatile constituents of different organs of *Psoralea bituminosa* L. *Flavour. Fragr. J.* **19**, 166–171 (2004).
- Lemouchi, R. et al. Chemical composition and antioxidant activity of essential oil and hydrosol extract obtained by hydrodistillation (HY) and liquid-liquid extraction (LLE) of *Psoralea bituminosa*. *J. Herbs Spices Med. Plants.* **23**, 299–307 (2017).
- Walker, D. J., Bernal, M. P. & Correal, E. The influence of heavy metals and mineral nutrient supply on *Bituminaria bituminosa*. *Water Air Soil. Pollut.* **184**, 335–345 (2007).
- Pistelli, L. et al. Arbuscular mycorrhizal fungi alter the content and composition of secondary metabolites in *Bituminaria bituminosa* L. *Plant. Biol.* **19**, 926–933 (2017).
- Bourgaud, F., Nguyen, C. & Guckert, A. *Psoralea* species: in vitro culture and production of furanocoumarins and other secondary metabolites. 388–411 https://doi.org/10.1007/978-3-662-08612-4_22 (1995).

6. Llorent-Martinez, E. J., Spinola, V., Gouveia, S. & Castilho, P. C. HPLC-ESI-MSⁿ characterization of phenolic compounds, terpenoid saponins, and other minor compounds in *Bituminaria bituminosa*. *Ind. Crops Prod.* **69**, 80–90 (2015).
7. Azzouzi, S. et al. Phytochemical and biological activities of *Bituminaria bituminosa* L. (Fabaceae). *Asian Pac. J. Trop. Med.* **7**, S481–S484 (2014).
8. Alagona, G., Ghio, C. & Monti, S. B3LYP/6-31G* conformational landscape in vacuo of some pterocarpin stereoisomers with biological activity. *Phys. Chem. Chem. Phys.* **6**, 2849–2857 (2004).
9. Koul, B., Taak, P., Kumar, A., Kumar, A. & Sanyal, I. Genus *Psoralea*: A review of the traditional and modern uses, phytochemistry and pharmacology. *J. Ethnopharmacol.* **232**, 201 (2018).
10. Al Ayoubi, S., Raafat, K., El-Lakany, A. & Aboul-Ela, M. Phytochemical investigation of *Psoralea bituminosa* L. and its anti-diabetic potentials. *Pharmacogn. J.* **10**, 841–853 (2018).
11. Francisco, M., Carrea, M. E., Butrón, A. M., Sotelo, T. & Velasco, P. Environmental and genetic effects on yield and secondary metabolite production in *Brassica rapa* crops. *J. Agric. Food Chem.* **60**, 5507–5514 (2012).
12. Ghasemian, A., Al-Marzoqi, A. H., Mostafavi, S. K. S., Alghanimi, Y. K. & Teimouri, M. Chemical composition and antimicrobial and cytotoxic activities of *Foeniculum vulgare* mill essential oils. *J. Gastrointest. Cancer.* **51**, 260–266 (2020).
13. Aboalhaja, N. et al. Phytochemical screening and cytotoxic evaluation of *Salvia greggii* extracts: an in vitro and in Silico study. *Farmacia* **72**, 171–177 (2024).
14. Aboalhaja, N. et al. Phytochemistry and antiproliferative potential of a naturalized plant to Jordan: *Lavandula stoechas*. *Chem. Biodivers.* **e202500181**, (2025).
15. Chan, J. C. Y., Kioh, D. Y. Q., Yap, G. C., Lee, B. W. & Chan, E. C. Y. A novel LCMSMS method for quantitative measurement of short-chain fatty acids in human stool derivatized with 12 C- and 13 C-labelled aniline. *J. Pharm. Biomed. Anal.* **138**, 43–53 (2017).
16. Youssif, Y. M., Ragab, A., Zahran, M. A., Ahmed, F. A. & Elhagali, G. A. Applying UPLC-QTOF-MS/MS to profile the phytochemical constituents associated with docking studies of major components of *Ziziphora capitata* L. as well as antimicrobial and antioxidant activity assessments of its subsequent fractions. *Discov Appl. Sci.* **6** (8), 385 (2024).
17. Awwad, O. et al. Chromatographic (LC-MS and GC-MS) and biological (antiproliferative) evaluation of a naturalized plant in Jordan: *Parkinsonia aculeata* L. *J. Herb. Med.* **39**, 100659 (2023).
18. Youssif, Y. M., Elhagali, G. A., Zahran, M. A., Ahmed, F. A. & Ragab, A. Utilising UPLC-QTOF-MS/MS to determine the phytochemical profile and in vitro cytotoxic potential of *Ziziphora capitata* L. with molecular docking simulation. *Nat. Prod. Res.* **1–9** (2024).
19. De Jager, L. S., Perfetti, G. A. & Diachenko, G. W. Comparison of headspace-SPME-GC-MS and LC-MS for the detection and quantification of coumarin, vanillin, and ethyl vanillin in vanilla extract products. *Food Chem.* **107** (4), 1701–1709 (2008).
20. Braunberger, C. et al. LC-NMR, NMR, and LC-MS identification and LC-DAD quantification of flavonoids and ellagic acid derivatives in *Drosera peltata*. *J. Chromatogr. B.* **932**, 111–116 (2013).
21. Heinonen, S. et al. Studies of the in vitro intestinal metabolism of isoflavones aid in the identification of their urinary metabolites. *J. Agric. Food Chem.* **52**, 2640–2646 (2004).
22. Martorana, A. et al. A spectroscopic characterization of a phenolic natural mediator in the laccase biocatalytic reaction. *J. Mol. Catal. B: Enzym.* **97**, 203–208 (2013).
23. Shajib, M. T. I., Pedersen, H. A., Mortensen, A. G., Kudsk, P. & Fomsgaard, I. S. Phytotoxic effect, uptake, and transformation of biochanin A in selected weed species. *J. Agric. Food Chem.* **60** (43), 10715–10722 (2012).
24. Yang, J., Saggiomo, V., Velders, A. H., Stuart, C. & Kamperman, M. M. A., Reaction pathways in catechol/primary amine mixtures: a window on crosslinking chemistry. *PLoS ONE.* **11** (12), e0166490 (2016).
25. Lin, L. et al. LC-ESI-MS study of the flavonoid glycoside malonates of red clover (*Trifolium pratense*). *J. Agric. Food Chem.* **48**, 354–365 (2000).
26. RDKit. <https://www.rdkit.org> (Accessed 19 Sept 2023).
27. Alvascience. AlvaDesc (Software for Molecular Descriptors Calculation) Version 1.0.18. <https://www.alvascience.com> (2020).
28. Nakashima, T. et al. 2,3,4-Trisubstituted acyl glucosides isolated from *Solanum pennellii*. *J. Nat. Prod.* **83**, 2337–2346 (2020).
29. Nusinow, D. P. et al. Quantitative proteomics of the cancer cell line encyclopedia. *Cell* **180**, 387–402e16 (2020).
30. Gao, J. et al. Integrative analysis of complex cancer genomics and clinical profiles using the cBioPortal. *Sci. Signal* **6**, (2013).
31. Park, G. H., Sung, J. H., Song, H. M. & Jeong, J. B. Anti-cancer activity of *Psoralea fructus* through the downregulation of Cyclin D1 and CDK4 in human colorectal cancer cells. *BMC Complement. Altern. Med.* **16**, 1–8 (2016).
32. Whelan, L. C. & Ryan, M. F. Ethanol extracts of *Euphorbia* and other ethnobotanical species as inhibitors of human tumour cell growth. *Phytomedicine* **10**, 53–58 (2003).
33. del Jacobo-Salcedo, M. R. et al. Antimicrobial and cytotoxic effects of Mexican medicinal plants. **6**, 1925–1928 (2011).
34. D'Angiolillo, F. et al. In vitro cultures of *Bituminaria bituminosa*: pterocarpin, furanocoumarin and isoflavone production and cytotoxic activity evaluation. *J. Agric. Food Chem.* **9**, 477–480 (2014).
35. Althaher, A. R., Shehabi, R. F., Ameen, H. H., Awadallah, M. W. & Mastinu, A. *Calamintha incana* methanolic extract: Investigation of phytochemical composition and antioxidant and antibacterial activities. *J. Food Biochem.* **2024**, 6634969 (2024).
36. Zafar, R. et al. A novel bioactive multifunctional compound from nature. *Sci. Total Environ.* **722**, (2020).
37. Li, Y. et al. Biochanin A induces S phase arrest and apoptosis in lung cancer cells. *Biomed. Res. Int.* **2018**, 3545376 (2018).
38. Szychowski, K. A., Rybczyńska-Tkaczyk, K., Leja, M. L., Wójtowicz, A. K. & Gmiński, J. Tetrabromobisphenol A (TBBPA)-stimulated reactive oxygen species (ROS) production in cell-free model using the 2',7'-dichlorodihydrofluorescein diacetate (H2DCFDA) assay—limitations of method. *Environ. Sci. Pollut. Res.* **23**, 12246–12252 (2016).
39. Lin, Y. J. et al. *Puerariae radix* isoflavones and their metabolites inhibit growth and induce apoptosis in breast cancer cells. *Biochem. Biophys. Res. Commun.* **378**, 683–688 (2009).
40. Janicke, B. et al. The antiproliferative effect of dietary fiber phenolic compounds ferulic acid and p-coumaric acid on the cell cycle of Caco-2 cells. *Nutr. Cancer.* **63**, 611–622 (2011).
41. Lee, D. E. et al. 7,3',4'-trihydroxyisoflavone, a metabolite of the soy isoflavone Daidzein, suppresses ultraviolet B-induced skin cancer by targeting Cot and MKK4. *J. Biol. Chem.* **286**, 14246–14256 (2011).
42. Alqub, M. & Jaradat, N. In vitro studies of *Bituminaria bituminosa* L. extracts from Palestine for their antioxidant, qualitative, and quantitative properties. *Palest. Med. Pharm. J.* **8**, 8 (2023).
43. Ramli, I. et al. In vitro and in vivo bioactivities of *Ambrosia maritima* and *Bituminaria bituminosa* organic extracts from Algeria. *J. Infect. Dev. Ctries.* **16**, 1064–1074 (2022).
44. Aboalhaja, N. H. et al. Chemodiversity and antiproliferative activity of the essential oil of *Schinus molle* growing in Jordan. *Chem. Biodivers.* **16**, e1900388 (2019).
45. AİBÜ Campus Flora. <http://ibufiora.ibu.edu.tr/en/species/bituminaria-bituminosa>.
46. Aboalhaja, N. H. et al. Chemical evaluation, in vitro and in vivo anticancer activity of *Lavandula angustifolia* grown in Jordan. <https://doi.org/10.3390/molecules27185910> (2022).
47. Abaza, I., Aboalhaja, N., Alsalman, A., Talib, W. & Afifi, F. Aroma profile, chemical composition and antiproliferative activity of the hydrodistilled essential oil of a rare *Salvia* species (*Salvia greggii*). *J. Biol. Act. Prod.* **11**, 129–137 (2021).
48. Al-Merini, M. A. et al. Chromatographic analysis (LC-MS and GC-MS), antioxidant activity, total phenol and total flavonoid determination of *Ononis natrix* L. grown in Jordan. *Jordan J. Chem.* **16**, 31–39 (2021).

49. Hajjo, R., Setola, V., Roth, B. L. & Tropsha, A. Chemocentric informatics approach to drug discovery: identification and experimental validation of selective estrogen receptor modulators as ligands of 5-hydroxytryptamine-6 receptors and as potential cognition enhancers. *J. Med. Chem.* **55**, 5704–5719 (2012).
50. Hajjo, R., Sabbah, D. A. & Bardaweel, S. K. Chemocentric informatics analysis: dexamethasone versus combination therapy for covid-19. *ACS Omega*. **5**, 29765–29779 (2020).
51. Bardaweel, S. K., AlOmari, R. & Hajjo, R. Integrating computational and experimental chemical biology revealed variable anticancer activities of phosphodiesterase isoenzyme 5 inhibitors (PDE5i) in lung cancer. *RSC Med. Chem.* **15**, 2882–2899 (2024).
52. Hajjo, R. & Tropsha, A. A systems biology workflow for drug and vaccine repurposing: identifying small-molecule BCG mimics to reduce or prevent COVID-19 mortality. *Pharm. Res.* **37**, 1–15 (2020).
53. Doncheva, N. T., Morris, J. H., Gorodkin, J. & Jensen, L. J. Cytoscape StringApp: network analysis and visualization of proteomics data. *J. Proteome Res.* **18**, 623–632 (2019).

Author contributions

N.H. conceptualization, chemistry and antiproliferative methodology, software, validation, prepared Figs. 1 and 2, writing, review and editing; R.H. computational analysis, software, validation, prepared Figs. 3, 4 and 5, writing, review and editing; F.A. conceptualization, writing, review and editing; H.S. chemistry methodology; R.A. antiproliferative methodology.

Funding

This work was funded by the Deanship of Scientific Research and Innovation at Al-Zaytoonah University of Jordan (2022–2023/07/23, 2022–2023/17/50 and 2024–2025/06/29).

Declarations

Competing interests

The authors declare no competing interests.

Additional information

Correspondence and requests for materials should be addressed to N.H.A.

Reprints and permissions information is available at www.nature.com/reprints.

Publisher's note Springer Nature remains neutral with regard to jurisdictional claims in published maps and institutional affiliations.

Open Access This article is licensed under a Creative Commons Attribution-NonCommercial-NoDerivatives 4.0 International License, which permits any non-commercial use, sharing, distribution and reproduction in any medium or format, as long as you give appropriate credit to the original author(s) and the source, provide a link to the Creative Commons licence, and indicate if you modified the licensed material. You do not have permission under this licence to share adapted material derived from this article or parts of it. The images or other third party material in this article are included in the article's Creative Commons licence, unless indicated otherwise in a credit line to the material. If material is not included in the article's Creative Commons licence and your intended use is not permitted by statutory regulation or exceeds the permitted use, you will need to obtain permission directly from the copyright holder. To view a copy of this licence, visit <http://creativecommons.org/licenses/by-nc-nd/4.0/>.

© The Author(s) 2025